# Effect of Sea Anemone Toxins on the Sodium Inactivation Process in Crayfish Axons

AKIRA WARASHINA and SHOZO FUJITA

From the Department of Physiology, Niigata University School of Medicine, and the Department of Neurochemistry, Brain Research Institute, Niigata University, Niigata, 951 Japan

ABSTRACT  The effect of sea anemone toxins from *Parasicyonis actinostoloides* and *Anemonia sulcata* on the Na conductance in crayfish giant axons was studied under voltage-clamp conditions. The toxin slowed the Na inactivation process without changing the kinetics of Na activation or K activation in an early stage of the toxin effect. An analysis of the Na current profile during the toxin treatment suggested an all-or-none modification of individual Na channels. Toxin-modified Na channels were partially inactivated with a slower time course than that of the normal inactivation. This slow inactivation in steady state decreased in its extent as the membrane was depolarized to above −45 mV, so that practically no inactivation occurred at the membrane potentials as high as +50 mV. In addition to inhibition of the normal Na inactivation, prolonged toxin treatment induced an anomalous closing in a certain population of Na channels, indicated by very slow components of the Na tail current. The observed kinetic natures of toxin-modified Na channels were interpreted based on a simple scheme which comprised interconversions between functional states of Na channels. The voltage dependence of *Parasicyonis* toxin action, in which depolarization caused a suppression in development of the toxin effect, was also investigated.

## INTRODUCTION

Polypeptide toxins have been extracted from sea anemones of various species. The fundamental action of the toxins on excitable membranes is similar to that of scorpion toxins, slowing the falling phase of action potential with no significant change in the resting potential in an early stage and provoking spontaneous firings in an advanced stage (Shapiro and Lilleheil, 1969; Rathmayer and Beress, 1976; Fujita and Warashina, 1980). It has been revealed by voltage-clamp experiments that sea anemone toxins (Narahashi et al., 1969; Bergman et al., 1976; Conti et al., 1976; Romey et al., 1976; Pelhate et al., 1979) as well as scorpion toxins specifically suppress the Na inactivation. This accounts for the prolongation of action potential in axons treated with these

toxins. In addition to such electrophysiological studies, binding characteristics of isotopically labeled polypeptide toxins to Na channels in various membranes have been extensively investigated under various conditions (Catterall, 1977; Okamoto, 1980; Vincent et al., 1980). Thus, this class of toxins has gained attention as a useful tool to investigate the molecular mechanism of Na channel function.

Recently, a sea anemone toxin (PaTX) from *Parasicyonis actinostoloides* was included in the class as a new member (Ishikawa et al., 1979), and basic characteristics of the toxin action have been studied (Ishikawa et al., 1979; Fujita and Warashina, 1980). It was shown in a previous study (Warashina et al., 1981) that the development of PaTX action was largely suppressed when applied to depolarized axons. In the present study the effect of PaTX or ATX II (toxin II from *Anemonia sulcata*) on the Na inactivation was further investigated using crayfish giant axons under voltage-clamp conditions to clarify the nature of toxin action, including the voltage-dependent PaTX effect and the specific mode of modification of the Na inactivation.

## MATERIALS AND METHODS

*Parasicyonis* toxin (PaTX) was extracted from the sea anemone *Parasicyonis actinostoloides*, collected at the Misaki Marine Biological Station of Tokyo University at Miura, Japan. The purification of PaTX was carried out by a method described by Ishikawa et al. (1979). PaTX consisted of a single band of polyacrylamide gel electrophoresis (Fujita and Warashina, 1980). Toxin II from *Anemonia sulcata* (ATX II) was purchased from Ferring GmbH (Kiel, Federal Republic of Germany). The purity of ATX II was certified to be 95% by the manufacturer and used without further purification.

Medial giant axons of 150–200 $\mu$m diam in the circumesophageal connectives of the crayfish *Procambarus clarkii* were separated from connective tissues and small fibers to use in voltage-clamp experiments. Van Harreveld's solution (V-H solution) containing (mM) 207 NaCl, 5.4 KCl, 13.5 $CaCl_2$, 5.3 $MgCl_2$, and 10 Tris-HCl (pH 7.4) was used as a standard medium of the axon. To suppress K current, 3-aminopyridine (Sigma Chemical Co., St. Louis, MO) was added to V-H solution at a concentration of 0.75 mM. When the toxin was dissolved in V-H solution, bovine serum albumin (0.5 mg/ml) was added to the solution to protect the toxin from adsorption to the surfaces of glass and perfusing tubings (Ishikawa et al., 1979). The molar concentration of PaTX was calculated in this study using 3,400 as the molecular weight that was obtained in a study analyzing the amino acid sequence of PaTX (Dr. N. Tamiya, personal communication; this value is tentative because the study has not been completed). The above value is considerably larger than those (~2,100 mol wt) estimated by column chromatography and gel electrophoresis in previous studies (Ishikawa et al., 1979; Fujita and Warashina, 1980). Since the molar concentration of PaTX mentioned in previous studies (Fujita and Warashina, 1980; Warashina et al., 1981) was based on the latter value, it must be read after correcting by a factor of 0.62 in these papers.

Voltage-clamp experiments were performed by a method schematically illustrated in Fig. 1. A portion of axon existing in the constriction (~400 $\mu$m in width) of the central pool formed in a Lucite chamber was isolated, as an artificial "node," from two lateral pools filled with 256 mM KCl by vaseline seals (shaded areas). The exterior of the axon in the constriction was continuously perfused with the V-H solution or appropriate solutions at a flow rate of 0.5 ml/min as usual using a

peristaltic pump. The temperature of the bath was kept at 12°C by bringing it into contact with a thermoelectric module (HTM-2024; Sharp Co., Osaka, Japan). The membrane potential at the node was measured by impaling the axon with a glass capillary microelectrode (M) filled with 3 M KCl. The current to clamp the membrane potential was fed through Ag-AgCl electrodes, two of which in the lateral pools were connected to the output of amplifier B and one in the central pool to ground. The holding potential was −100 mV unless otherwise stated. Axons at this holding potential were slightly hyperpolarized from the natural resting potential (about −85
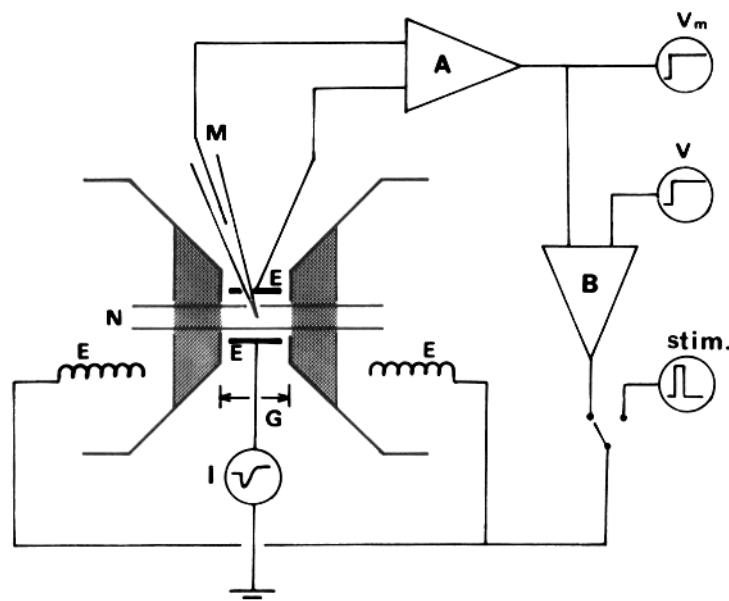


FIGURE 1.   Diagrammatical representation of a voltage-clamp method. A small portion of cleaned giant axon (N) of the crayfish was isolated in a 400-$\mu$m constriction (G) of the central pool by bilateral vaseline seals (shaded portions). The lateral pools were filled with 256 mM KCl. The axon in the constriction was perfused with V-H solution and impaled by a glass capillary microelectrode (M) for monitoring the membrane potential. E: Ag-AgCl electrodes; A: differential amplifier for the potential measurement; B: voltage-clamp amplifier; $V_m$: membrane potential; $V$: command voltage; $I$: membrane current; stim: stimulus for evoking the action potential.

mV). In this way, better consistency can be provided in the relation between PaTX concentration and the rate of toxin action than when axons are clamped at the resting potential. Near the normal resting potential, PaTX action is influenced by small changes of membrane potential, making the results variable.

The leakage current in the present case consists of two components. One is the membrane leak current, which exists after the complete block of voltage-sensitive ion channels by both tetrodotoxin (TTX) and 3-aminopyridine. The other flows longitudinally in the extracellular space under the vaseline covers. As analyzed by New and Trautwein (1972), a part of longitudinal leak current causes the membrane

current, when it appears at a detector, to be magnified $[1 + (r_{ig}/r_{eg})]$ times without distorting its waveform, where $r_{eg}$ and $r_{ig}$ are the longitudinal extracellular and intracellular resistances at the vaseline seals, respectively. The above factor is equal to the amplitude ratio of the action potential recorded intracellularly to that recorded extracellularly (Julian et al., 1962), ranging from 1.2 to 1.5 in the present case. The measured intensity of membrane current was corrected here according to the ratio. The linear portion of leakage and capacitative currents was usually canceled from the current record using a signal averager (ATAC 250; Nihon Kohden Co., Tokyo) by a sequential addition of the response obtained with a depolarizing pulse to that obtained with an exact reverse of it. The error caused by the resistance in series with the membrane was partially corrected by a compensated feedback. The distortion of the current profile caused by the series resistance was not serious when checked under the condition of a reduced Na current density in the presence of 2 nM TTX.

The method of voltage clamp described above is similar to that reported by New and Trautwein (1972). However, the advantage of the present method is as follows: the bilateral current injection provides a symmetrical current flow through the membrane, so that a relatively large area of membrane is stably space-clamped compared with the one-sided current injection in the above-mentioned version or in the usual gap methods (Julian et al., 1962; Frankenhaeuser et al., 1966).

## RESULTS

### Effect of PaTX on Na Current

The early stage of PaTX action is characterized by a prolongation of the duration of action potential without significantly changing the resting potential and rate of rise (Fujita and Warashina, 1980). In the experiment of Fig. 2, an axon was treated with 50 nM PaTX for 5 min and the development of toxin action was stopped by removing PaTX in the bath by perfusion. The following perfusion of the axon with toxin-free V-H solution did not alter the level of the toxin action thereby obtained. A change in the action potential by the above treatment is shown in the inset of Fig. 2. The corresponding change in current profile under voltage clamp was recorded with a step depolarization to −16 mV from the holding potential of −100 mV and represented by traces *a* and *b* in Fig. 2, which were taken before and after the PaTX treatment, respectively. The outward steady state current observed initially was reversed inwardly by the toxin effect. A block of Na current by 100 nM TTX revealed the K current profile (trace *c*). The steady state level of K current was not altered from that obtained with the untreated axon. This indicates that PaTX, like other sea anemone toxins (Narahashi et al., 1969; Bergman et al., 1976; Romey et al., 1976) and scorpion toxins, selectively slows Na inactivation process while the Na activation or the steady state K conductance remains unaltered in an early stage of the toxin effect.

The voltage dependence of Na and K currents at different stages of the experiment of Fig. 2 are summarized in Fig. 3. The activation of Na conductance in the normal axon takes place around −70 mV as read from a break in the *I-V* curve of peak inward current indicated by the solid line through the open circles. The corresponding value obtained by Shrager (1974) was reported to be −50 mV. A major point of discrepancy, however, seems to be created by

the different holding potentials used in both experiments since an *I-V* relation very similar to that found by Shrager was observed in our laboratory when the axon was clamped at −80 mV instead of −100 mV. The increase in intensity of peak inward current by PaTX (filled circles) was observed in our experiments. The K current in the PaTX-treated axon measured after TTX application (crosses) deviated slightly in the higher potential from that of untreated axons (triangles). This, however, may not be significant since the extent and direction (either increase or decrease) of the deviation varied from experiment to experiment. The difference between the currents in PaTX-treated axon before (trace *b* in Fig. 2) and after the TTX application (trace *c*)
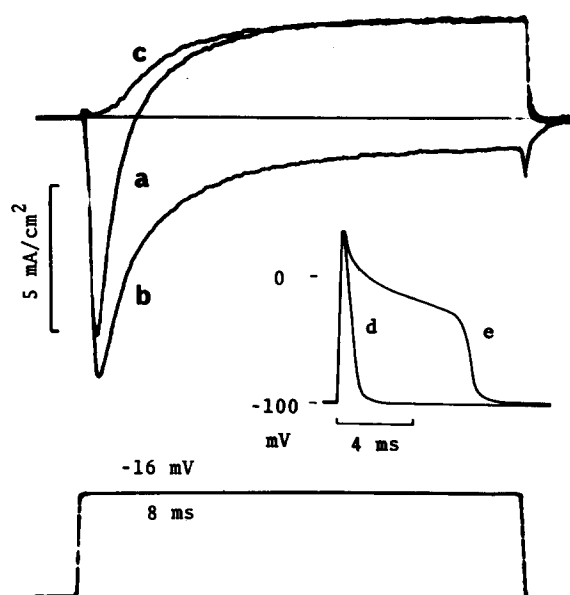


Figure 2.   Effect of PaTX on the membrane current associated with a depolarizing pulse to −16 mV from the holding potential of −100 mV. (*a*) Before treatment (control); (*b*) after a 5-min treatment of the axon with 50 nM PaTX; (*c*) after application of 100 nM TTX to the axon used for *b*. (Inset) Action potentials, *d* and *e*, were recorded shortly before measuring *a* and *b*, respectively. The resting potential was set at −100 mV by current injection.

was taken at the end of an 8-ms depolarizing pulse; the intensity of PaTX-induced steady state current is shown by the filled squares in Fig. 3.

The voltage dependence of PaTX-induced steady state Na current is different from that of the peak inward current (filled circles), showing a maximum around −15 mV for the former and around −45 mV for the latter. A similar characteristic has been reported with scorpion toxin (Narahashi et al., 1972; Gillespie and Meves, 1980). The reversal point of peak current obtained either before or after the PaTX treatment roughly coincides with that of the PaTX-induced steady state current, although the latter tended to reverse at the potential of few millivolts higher than the former.

*Time Course of Na Current in PaTX-treated Axons*

To study the time course of Na current in detail under the influence of the toxin, K current was blocked by 0.75 mM 3-aminopyridine (Yeh et al., 1976) throughout the following experiments. The development of steady state Na current by 50 nM PaTX is depicted in Fig. 4. The effect was practically saturated at ~26 min after commencement of the treatment. A residual, slow
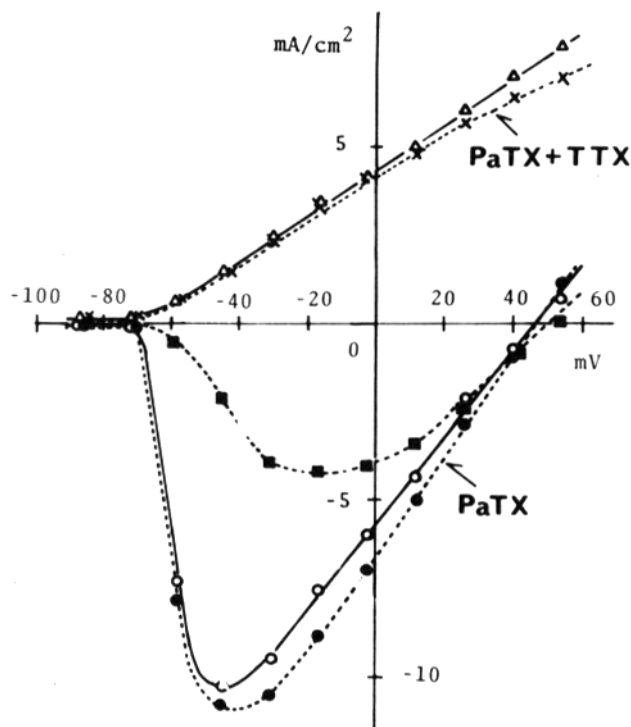


FIGURE 3. Current-voltage relationship in an axon before or after treatment with 50 nM PaTX for 5 min. Symbols: peak sodium current before (○) or after (●) the PaTX treatment; the steady state potassium current before (△) the PaTX treatment or after (✕) 100 nM TTX application to the PaTX-treated axon; the PaTX-induced steady state sodium current (■), given by subtraction of the potassium current (✕) from the steady state current in the PaTX-treated axon.

inactivation seen at such a stage could not be eliminated even by a longer exposure of an axon with more concentrated PaTX. It was shown from traces on longer time bases that the slow inactivation progressed exponentially with a time constant of ~3.5 ms. The steady state current that is left after the partial, slow inactivation was not literally steady but declined very slowly with a time constant of several hundred milliseconds.

Of the conceivable modes of toxin action, the simplest may be an all-or-none modification of individual Na channels through the toxin binding to them. In that case the intermediate traces in Fig. 4 may be reconstructed by a linear combination of the two extremes; one is the current profile at 0 min for a contribution of intact channels and the other is that at 26 min for PaTX-poisoned channels. Since the reconstruction represented by the dots in Fig. 4 satisfactorily simulates the recorded current profiles (solid lines), an all-or-none modification of the conducting state of each Na channel by the toxin may be the case.

The extent of the increase in the peak inward current after removal of the normal inactivation by PaTX was measured with a depolarizing step to $-16$
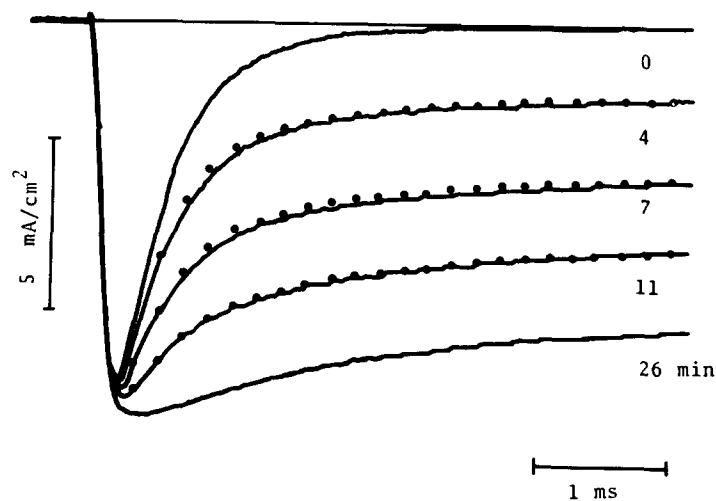


FIGURE 4.   Time courses of the sodium current during treatment of an axon with 50 nM PaTX. Current records taken with depolarizing voltage steps to $-16$ mV from the holding potential of $-100$ mV are superimposed. The time from the onset of treatment is indicated at each record. Dots along the experimental records were calculated by addition of the two records at 0 and 26 min in appropriate ratios for the respective cases. The external medium contained 0.75 mM 3-aminopyridine to block the potassium current.

mV, and in 15 experiments was 15 ± 7% (SD) of the control. In the Hodgkin-Huxley scheme (Hodgkin and Huxley, 1952), the inactivation with an exponential decay begins immediately after an applied depolarization so that a substantial degree of inactivation takes place at the peak of Na conductance, e.g., an 86% increase in the peak Na current would have been expected in the case of Fig. 4 by complete removal of inactivation. One of the possible explanations for the small increase observed may be given by a coupled activation-inactivation mechanism of Na channel gating, such as that originally proposed by Bezanilla and Armstrong (1977) for a pronase-treated axons.

*Development of Steady State Na Current*

Time courses of the increase in steady state Na current intensity when axons were treated with various concentrations of PaTX are presented in Fig. 5. The initial lag of toxin action was simply caused by the time required to replace the medium with a solution containing PaTX and for the toxin to diffuse to the axonal membrane. Apart from the lag, the curves were fitted by a function of $[1 - \exp(-kt)]$, where $t$ is the time from the onset of PaTX treatment (after correcting for the initial lag) and $k$ is a constant determined by toxin concentration. This suggests a direct relation between the development in steady state Na current by PaTX treatment and the increase in PaTX
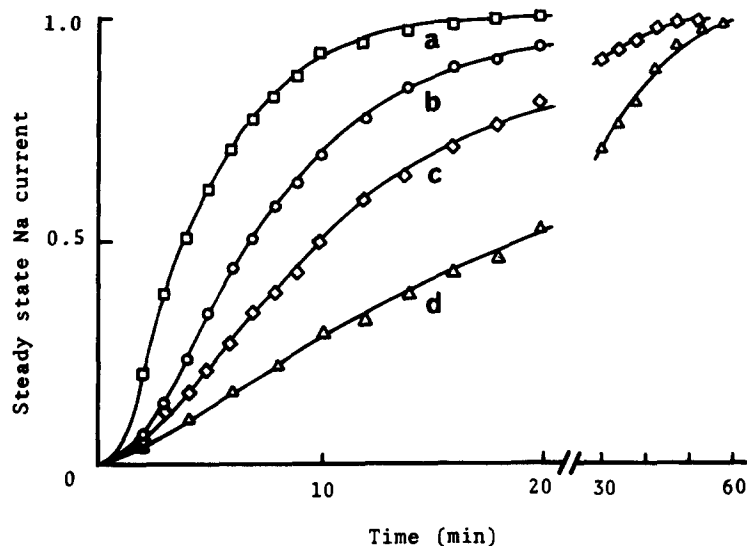


FIGURE 5. Time course of development of the steady state Na current during PaTX treatment. The time from the onset of the treatment is indicated on the abscissa. PaTX concentrations used were (a) 100 nM, (b) 50 nM, (c) 25 nM, and (d) 13 nM. The current intensity measured at the end of an 8-ms depolarizing pulse to −16 mV was plotted after it was normalized to its saturated level in each experiment.

binding to saturable sites in the membrane, which can also be expressed by the above exponential function with the following rate constant:

$$k = \alpha[\text{toxin}] + \beta,$$

where $\alpha$ and $\beta$ are the association and dissociation rate constants, respectively, and [toxin] is the concentration of toxin. Values of $k$ evaluated from experimental data including those in Fig. 5 were roughly proportional to the toxin concentration in the range from 100 to 6 nM. No component for the normal, fast inactivation was apparently found even in the current profile recorded from an axon treated with the lowest PaTX concentration examined (6 nM).

The results are readily understood if the dissociation rate constant, $\beta$, is negligibly small compared with $\alpha$[toxin] in this concentration range. The value of $\alpha$ thus evaluated was $5.5 \times 10^4$ $(M \cdot s)^{-1}$.

A slow dissociation rate was indicated by the fact that the level of steady state Na current attained after PaTX tretment was kept unaltered during a 40-min washing of the axon with toxin-free V-H solution. Because a 4% change in the current level was detectable in the measurement, the dissociation rate constant, $\beta$, must be smaller than $1.7 \times 10^{-5}$ $s^{-1}$. Thus, the equilibrium dissociation constant, $K_d = \beta/\alpha$, for PaTX binding to the crayfish giant axon is lower than 0.3 nM. However, it is noted that the above evaluation becomes
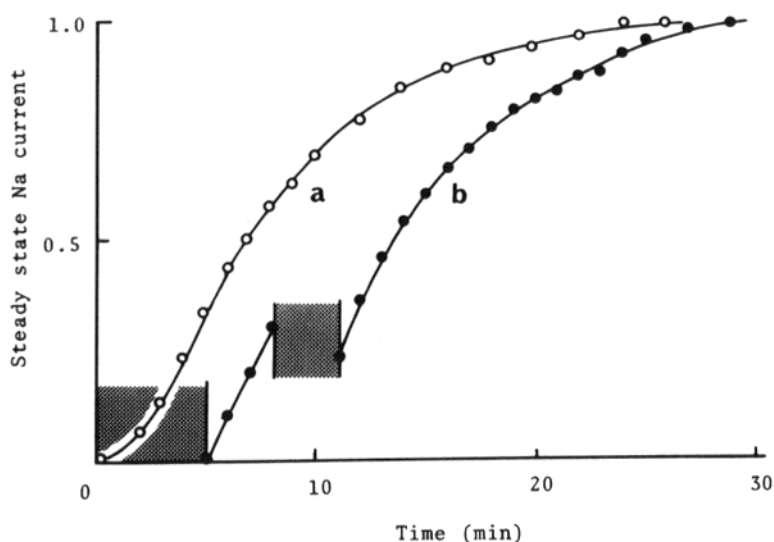


FIGURE 6.   Effect of membrane depolarization on the development of PaTX action. The steady state Na current relative to its saturated level was plotted vs. the time from the onset of treatments of axons with 50 nM PaTX; (*a*) transcription of *b* in Fig. 5; (*b*) the membrane was depolarized to −40 mV during periods of 0–5 and 8–11 min.

meaningless if the observed dissociation rate should appear very small merely as a result of reactions between a toxin molecule and its receptor sites, i.e., dissociated toxin molecules might be trapped in some axonal or peri-axonal structures and recaptured before they are washed out.

*Effect of Depolarization on Toxin Action*

In the experiment of Fig. 6 an axon was depolarized to −40 mV immediately after the onset of perfusion with 50 nM PaTX (curve *b*). After the membrane potential was returned from a 5-min depolarization to −40 mV to the holding potential, the steady state Na current started increasing as if the treatment had been commenced at this point. Obviously, the PaTX action was sup-

pressed under the imposed membrane depolarization. The initial lag seen in curve *a*, which was obtained without imposing depolarization, is absent in curve *b* because the replacement of the external medium and the accession of PaTX to the axonal membrane were well accomplished during the 5-min perfusion under depolarization. When the second depolarization to −40 mV from 8 to 11 min was removed, the level of steady state Na current was reduced slightly compared with that reached immediately before the depolarization as seen in the figure. However, it seems that most of the decrease in the current intensity was not caused by the dissociation of the toxin but to some aftereffect of the prolonged depolarization, which was indicated as a small fall (~5%) of peak Na current recognized in an original record (not shown here). The aftereffect might be related to the ultraslow inactivation (Fox, 1976) that is known to develop during a prolonged membrane depolarization. In a detailed experimental procedure, the first measurements following the depolarized periods (0–5 and 8–11 min) were carried out ~8 s after the removal of the depolarizations. The axon at those moments might have still been under the influence of the ultraslow inactivation. However, this does not account for a major portion of delay in the toxin action as shown in curve *b* (Fig. 6) because, except for one experimental point mentioned above, the peak levels of Na currents measured after the depolarizations did not show any decrease that indicated ultraslow inactivation. On the contrary, they increased slightly in a trend similar to that seen in Fig. 4. Thus, the observed delay in the toxin action is most adequately explained in terms of the potential-dependent toxin action (Mozhayeva et al., 1980; Warashina et al., 1981), which is presumably derived from the depolarization-induced inhibition of toxin binding to membrane sites (Catterall, 1977).

### Characteristics of Slow Inactivation

After the toxin effect was saturated by an extensive treatment, a residual inactivation with a time course one order of magnitude slower than that of the normal inactivation remains, as shown in Fig. 4. To examine the voltage dependence of the slow inactivation, the influence of 8-ms conditioning pulses on the level of Na current induced by a test pulse to −16 mV immediately after the conditioning pulse is measured as shown in Fig. 7A. The current density with a prepulse to −58 mV is slightly larger at the beginning than that to −16 mV (compare record *b* with *c*). However, the slow inactivation at −58 mV develops more extensively than that at −16 mV, so that the level of Na current at −58 mV becomes smaller than that at −16 mV in the later period of the prepulse. This suggests that the voltage dependence of slow inactivation is different from that of normal inactivation. When the membrane potential is stepped from −58 to −16 mV, an instantaneous drop in the current intensity occurs because of the decrease in driving force for Na ions, and a sharp recovery follows, probably because of the activation of the Na channels that have not been activated by the relatively small prepulse to −58 mV. After these rapid changes, the current intensity slowly increases toward the steady state level indicated by curve *a*, which was recorded with a step

depolarization to −16 mV without prepulse. This slow increase may be explained by a reopening of the inactivated Na channels that was produced as an excess fraction by the shift in the membrane potential, since the slow inactivation at the steady state is more extensive at −58 mV than at −16 mV, as mentioned above. The above observation suggests that the steady state level of Na conductance in the PaTX-treated axon may be equilibrated, depending merely on the voltage of the test pulse, regardless of the prepulse condition.
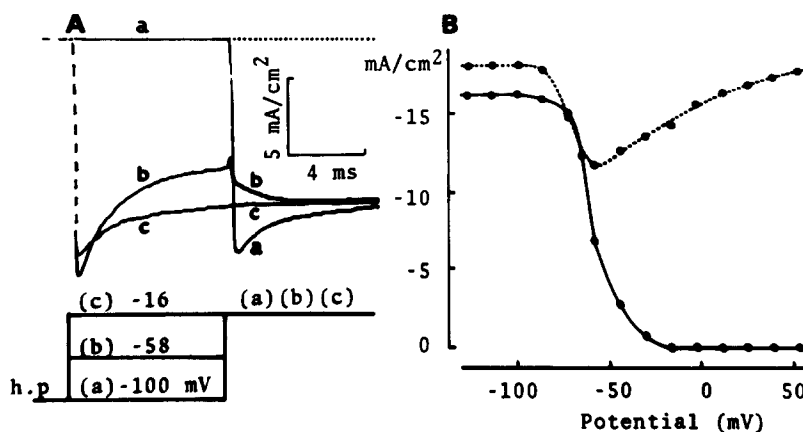


FIGURE 7.   Characteristics of the slow inactivation in a PaTX-treated axon. A. Current profiles during 8-ms conditioning prepulses to the indicated voltages and the subsequent test pulse to −16 mV. The holding potential (hp) was −100 mV. The axon was treated with 150 nM PaTX for 15 min. The dashed line on the extreme left of the panel was added artificially afterwards to the original records to help presentation. B. The peak inward currents (--●--) with the test pulse or extrapolated levels of the slow current component to the onset time of the test pulse were plotted as a function of the voltage of the conditioning prepulse in the PaTX-treated axon; intensities of the peak inward currents (-O-) measured with the test pulse after the conditioning prepulse in the axon before the toxin treatment. The external medium contained 0.75 mM 3-aminopyridine to block the potassium current.

Using the data shown in Fig. 7A and other results at various voltages of the prepulse, the voltage dependence of the slow Na inactivation in the PaTX-treated axon at the end of 8-ms prepulses is represented by the dotted line through the filled circles in Fig. 7B. In practice, these filled circles denote either peak Na current densities induced by the test pulse to − 16 mV after prepulses to various voltages indicated on the abscissa, or current levels determined by extrapolations of the slow changes at the beginning of the test pulse in cases such as that seen in record *b* (Fig. 7A). The slow inactivation so determined intensified as the level of depolarization increases in the voltage range from −85 to −45 mV. However, it decreases by further depolarization, so that no practical inactivation occurs at membrane potentials as high as

+50 mV. This contrasts sharply with the normal inactivation in an intact axon represented by the solid line through the open circles in Fig. 7B, which mark relative intensities of the peak Na current induced by the test pulse to −16 mV after 8-ms prepulses.

*Interconversion between Functional States of Na Channel*

Another aspect of the kinetic properties of PaTX-modified Na channels is seen in Fig. 8. When the membrane potential is altered from +40 mV (first step) to −65 mV (second step), the current intensity (record *b*) instantaneously increases to a level exceeding the maximum level in record *a*, which was taken with a step to −65 mV directly from the holding potential. This means that all Na channels were activated at +40 mV without being subjected to substantial inactivation (cf. Fig. 7B) and conducted a large current at the
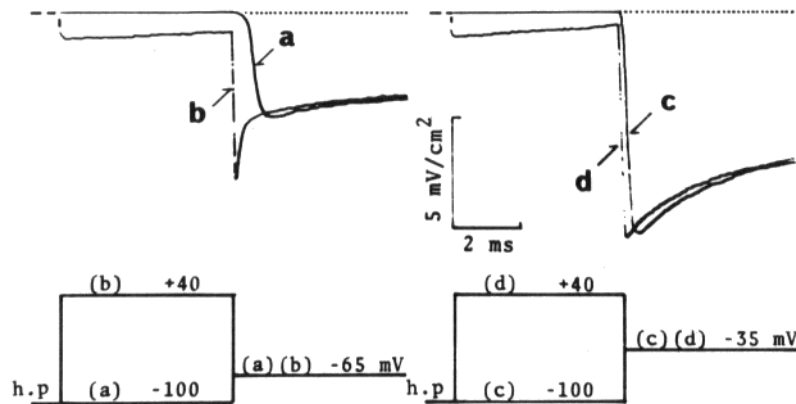


FIGURE 8.   Current profiles in a PaTX-treated axon during voltage clamp with various pulse programs from the holding potential (hp) of −100 mV. Letters assigned for the traces correspond to the pulse patterns. The measurements were carried out after a 15-min treatment of the axon with 150 nM PaTX. The external medium contained 0.75 mM 3-aminopyridine to block the potassium current.

beginning of the second step to −65 mV, where only a limited population of Na channels was activated if no prepulse was applied. A fast decrease following the instantaneous increase is shown in record *b* (Fig. 8), which implies that a fraction of activated Na channels returns rapidly to the unactivated state (the state before activation) without passing through the inactivated state. A remaining fraction of the activated channels was subjected to the slow inactivation to attain the steady state level for the membrane potential of −65 mV. The initial fast decrease became more rapid as the voltage of the second step was lowered. If, on the other hand, a higher voltage above −35 mV is used for the second step, no fast current component is observed because a very small fraction of Na channels would be converted into the unactivated state, as judged from Fig. 3. This is exemplified by record *d* in Fig. 8.

## Toxin Effect on Tail Current

An anomaly in the tail current at the end of the depolarizing pulse was seen in axons extensively treated with PaTX or ATX II as reported by Romey et al. (1975) with a scorpion toxin. Unlike the highly consistent toxin action on Na inactivation, the toxin effect on the tail current was somewhat irregular in its development and final extent, although the phenomenon itself was consistently seen with a variable delay from the onset of toxin treatment. Some typical characteristics of the anomaly are illustrated in Fig. 9. Record *a* in Fig. 9A was taken from an axon exposed to 20 nM ATX II for 12 min, in which
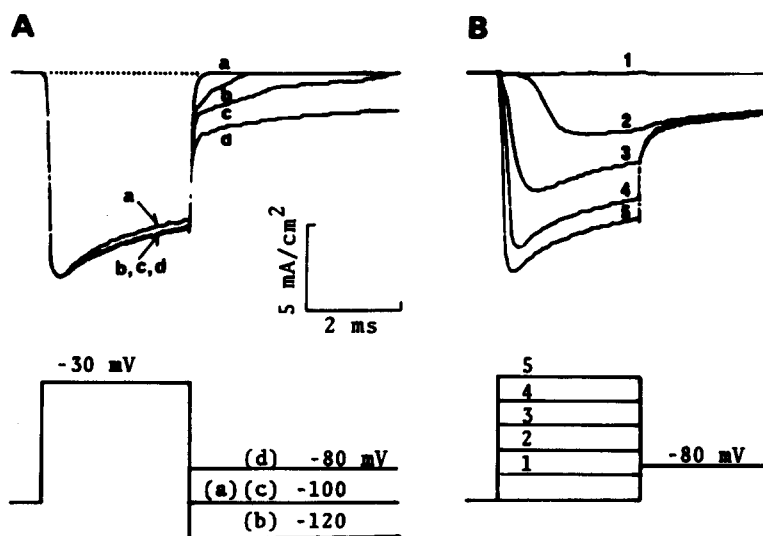


FIGURE 9.   Current profiles in an axon treated with 20 nM ATX II. A. (*a*) The sodium current associated with a depolarizing pulse to −30 mV after 13 min ATX II treatment; (*b-d*) anomalous tail currents occurring after 26 min of treatment on repolarizations from −30 mV prepulse to the membrane potentials of −120, −100, and −80 mV, respectively. B. The membrane potential was shifted to −80 mV after depolarizing pulses to (1) −86, (2) −72, (3) −58, (4) −44, and (5) −30 mV, respectively. The external medium contained 0.75 mM 3-aminopyridine to block the potassium current.

the tail current was not conspicuously distorted. After that period the anomaly developed rapidly toward a rather steady level, as shown by record *c* at 26 min. The decay time of conductance on repolarization became longer at a membrane potential of −80 mV (record *d*), whereas it was shortened at − 120 mV (record *b*). In Fig. 9B, the membrane potential was shifted to −80 mV after step depolarizations to various voltages from −86 to 30 mV. The anomalous tail current is invariant despite the increasing number of Na channels that were activated by the successive elevations in the depolarization level.

The toxin-induced anomalous tail current probably flows through Na channels since it was completely blocked by 100 nM TTX and was totally absent in the voltage range where Na channels were not activated, as seen in record 1 in Fig. 9B. It seems that a certain population of Na channels may be modified to slow the closing process. The same population may be activated at a lower threshold. In fact, in association with the occurrence of the anomalous tail current after toxin treatment, there was often a small group of channels that activated at a voltage negative to the normal threshold.

### Comparison of Toxin Actions of PaTX and ATX II

All the experiments with PaTX presented in Figs. 2–8 were also carried out with ATX II, and that with ATX II in Fig. 9 was conducted with PaTX. Although not many trials for such experiments have been performed, none of the essential aspects of the toxin action are so far recognized to be different between the two toxins, which suggests that the detailed mechanism of toxin action is identical in PaTX and ATX II.

### DISCUSSION

### General Aspects of the Toxin Action

It is shown in the present study that either PaTX or ATX II suppressed the Na inactivation without significantly altering the kinetics of Na activation or the steady state K conductance in an early stage of the toxin action, as reported with sea anemone toxins from *Condylactis gigantea* (Narahashi et al., 1969) and *Anemonia sulcata* (Romey et al., 1976), although the prolonged treatment of axons with those toxins induced anomalous kinetics on the Na activation. An all-or-none modification of Na inactivation was suggested as the most probable mode of toxin action from the analysis of Na current profiles during development of the poisoning (Fig. 4). One might assume that such a mode of modification is directly associated with saturable bindings of the toxins to receptor sites in the membrane, which has been demonstrated by isotopically labeled scorpion toxins (Catterall, 1977; Okamoto, 1980) and sea anemone toxins (Vincent et al., 1980; Stengelin and Hucho, 1980). The above notion is compatible with the fact that the steady state Na current in poisoned axons increased in a time- and concentration-dependent manner (Fig. 5), as expected from the saturable toxin binding. Thus, the toxin-induced steady state Na current density may be proportional to the population of toxin-modified Na channels. However, an uncertain aspect remains in the present study since the equilibrium dissociation constant ($K_d$) of PaTX binding was found to be so small that its exact value could not be obtained (<0.3 nM). A final conclusion should be reserved until the presumed relationship between steady state Na current and toxin binding is tested in parallel using isotopically labeled toxin.

### Potential-dependent Effect of PaTX

It was demonstrated in the experiment of Fig. 6 that a depolarized membrane potential caused a suppression in development of the toxin effect of PaTX.

The potential-dependent scorpion toxin effect on voltage-clamped myelinated nerves was reported by Mozhayeva et al. (1980). In their preparation, the toxin effect was reversible, so that an increase in the equilibrium association constant of the toxin binding as the axon was depolarized could be quantitatively analyzed by measuring the steady state Na current induced by the toxin.

Using isotopically labeled polypeptide toxins, suppressions of toxin binding to depolarized membranes have been investigated by Catterall (1977, 1979) and Vincent et al. (1980). Tamkun and Catterall (1981) demonstrated that Na channels extracted from rat brain synaptosomes lost binding affinity for scorpion toxin but restored it after they were reconstituted into lipid vesicles so as to be subjected to membrane potential.

Still unresolved is whether the membrane potential itself readily affects the toxin binding or some other factor, such as the potential-dependent conducting state of Na channel, is responsible for the phenomenon. A model proposed by Catterall (1977) can be cited as an example of the latter notion, in which the toxin affinity for its receptor is influenced by voltage-dependent conformations of a Na channel. The toxin binding brings abouts its toxicity, in Catterall's model, by inhibiting the conformational conversion from an activated state to an inactivated state under a depolarized membrane potential.

On the other hand, Barhanin et al. (1981) found that chemical modification of ATX II completely abolished the toxin action but left the affinity for binding sites unchanged. This may argue against Catterall's model because the toxin binding and the toxin action could be thought of as separable events.

*Kinetic Properties of Toxin-modified Na Channels*

It may be convenient to introduce the following simplified scheme for discussing kinetic properties of Na channels modified by toxin.

$$C_n \cdots C_1 \underset{j^-}{\overset{j^+}{\rightleftharpoons}} O \underset{k^-}{\overset{k^+}{\rightleftharpoons}} I^* \qquad\qquad \text{(I)}$$

In this scheme, interconversions between the closed $(C)$, open $(O)$, and inactivated $(I)$ states take place in normal Na channels according to voltage-dependent kinetic rates (the closed state is represented by multistates in the scheme to fit the Hodgkin-Huxley [1952] type of activation kinetics, as has been described by various investigators [Moore and Cox, 1976; Bezanilla and Armstrong, 1977], but described hereafter as a single state $C$ for convenience since the following discussion is not concerned with details of the activation process). When the Na channel function is modified by the toxin, the $O$-$I$-$C$ conversion is blocked, whereas the activation process ($C$-$O$ conversion) is little affected, at least in an early stage of the toxin action. A new state denoted by $I^*$ appears under toxin influence to give rise to the residual, slow inactivation as described in the previous section. Whether such a state is newly formed only after the toxin is bound or exists also in intact channels, being masked by the normal, fast inactivation, is open to question.

Three major time courses, fast, slow, and steady, were observed during the Na inactivation process in axons partially treated with PaTX (Fig. 4). By assuming the existence of two distinct populations of Na channels, one intact and the other toxin modified, the fast current component is ascribed to the $O$-$I$ conversion, whereas the slow and steady components is ascribed to $O$-$I^*$ conversion in scheme I. The intensity ratio between the slow and steady components is determined by an equilibrium constant, $K = k^+/k^-$, whereas the developing rate of slow inactivation is approximately given by $K = k^+$ $+ k^-$, where $k^+$ and $k^-$ are forward and backward rate constants of the $O$-$I^*$ conversion, respectively.

The interconversion between the three states in scheme I became evident when current profiles were recorded with voltage pulses immediately after conditioning pulses. The conversion from $I^*$ to $O$ was suggested in the current record (trace $b$ in Fig. 7) by shifting the membrane potential from $-58$ to $-16$ mV. On the other hand, it was suggested from trace $b$ in Fig. 8 that Na channels that existed exclusively in the $O$ state after activation by a prepulse to $+40$ mV were redistributed into the three ($C$, $O$, and $I^*$) states during the second voltage step to $-65$ mV. The $O$-$C$ conversion gave rise to the fast initial fall in the Na current, whereas the $O$-$I^*$ conversion generated the later slow current component.

It may be questioned whether there exists a direct pathway on the recovery from anomalous inactivation ($I^*$-$C$ conversion) other than the pathway through the open state $O$ which is described in scheme I. One might suggest that a precise analysis on the tail current could provide the answer to the question. However, this was disturbed by the occurrence of the anomalous tail current as shown in Fig. 9.

### Anomalous Tail Current Induced by Toxin

It seems that only a certain population of toxin-modified Na channels showed an abnormality in the closing process of Na channels. In the anomalous channels, the returning rate ($j^-$) from $O$ to $C$ on repolarization may be slowed without altering the rate ($j^+$) on activation. As a result, the threshold of Na activation is lowered in these channels as mentioned in the previous section.

Many aspects of the anomalous tail current induced by PaTX or ATX II resemble those shown by Meves et al. (1982) in the nodal membranes that were treated with some toxin components from the scorpion *Centruroides sculpturatus*. The toxin components from the scorpion venom also slowed the Na inactivation process, although the effect on the inactivation was less conspicuous than that on the activation (induction of the tail current). The above effectiveness sequence might be said to be opposite in its order to that of PaTX and ATX II. It is likely that this class of polypeptide toxins exerts the bifunctional actions both on the activation and inactivation processes. An alternative explanation for the present case, although it is less probable, may be that small contaminants in PaTX and ATX II are responsible for the induction of an anomalous tail current.

## Mechanism of Inhibition of Na Inactivation by Polypeptide Toxins

Various kinetic schemes have been proposed for interpreting experimental data obtained by different combinations of polypeptide toxins and nerve membranes (Bergman et al., 1976; Neumcke et al., 1980; Gillespie and Meves, 1980). Since these schemes, including the present one, differ from each other, further efforts should be made to determine whether a unified explanation that is applicable to all the cases exists.

Other than polypeptide toxins, various reagents are known to remove the Na inactivation completely or partially. Among them, the effects of pronase (Bezanilla and Armstrong, 1977) and N-bromoacetamide (Oxford et al., 1978) may be interestingly compared with those of polypeptide toxins including PaTX and ATX II, since the former reagents exhibit the action only when applied intracellularly, whereas the latter are effective only extracellularly (Narahashi et al., 1972; Romey et al., 1976). It seems, therefore, that the toxin binding to the outer membrane of axon can affect the inactivation mechanism of the Na channel that is located on the inner side of membrane either by interfering with a conformational change or by suppressing a charge movement (Bezanilla and Armstrong, 1977) that presumably takes place across the membrane under depolarization.

REFERENCES

Barhanin, J., M. Hugues, H. Schweitz, J. P. Vincent, and M. Lazdunski. 1981. Structure-function relationships of sea anemone toxin II from *Anemonia sulcata. J. Biol. Chem.* 256:5764–5769.

Bergman, C., J. M. Dubois, E. Rojas, and W. Rathmayer. 1976. Decreased rate of sodium conductance inactivation in the node of Ranvier induced by a polypeptide toxin from sea anemone. *Biochim. Biophys. Acta.* 455:173–184.

Bezanilla, F., and C. M. Armstrong. 1977. Inactivation of the sodium channel. I. Sodium current experiments. *J. Gen. Physiol.* 70:549–566.

Catterall, W. A. 1977. Membrane potential-dependent binding of scorpion toxin to the action potential $Na^+$ ionophore. *J. Biol. Chem.* 252:8660–8668.

Catterall, W. A. 1979. Binding of scorpion toxin to receptor site associated with sodium channels in frog muscle. *J. Gen. Physiol.* 74:357–391.

Conti, F., B. Hille, B. Neumcke, W. Nonner, and R. Stämpfli. 1976. Conductance of the sodium channel in myelinated nerve fibers with modified sodium channel inactivation. *J. Physiol. (Lond.).* 262:729–742.

Fox, J. M. 1976. Ultra-slow inactivation of the ionic currents through the membrane of myelinated nerve. *Biochim. Biophys. Acta.* 426:232–244.

Frankenhaeuser, B., B. D. Lindley, and R. S. Smith. 1966 Potentiometric measurement of membrane action potentials in frog muscle fiber. *J. Physiol. (Lond.).* 183:152–166.

Fujita, S., and A. Warashina. 1980. *Parasicyonis* toxin: effect on crayfish giant axon. *Comp. Biochem. Physiol.* 67C:71–74.

Gillespie, J. I., and Meves. 1980. The effect of scorpion venoms on the sodium currents of the squid giant axon. *J. Physiol. (Lond.).* 308:479–499.

Hodgkin, A. L., and A. F. Huxley. 1952. A quantitative description of membrane current and its application to conduction and excitation in nerve. *J. Physiol. (Lond.).* 117:500–544.

Ishikawa, Y., K. Onodera, and A. Takeuchi. 1979. Purification and effect of the neurotoxin from sea anemone, *Parasicyonis actinostoloides. J. Neurochem.* 33:69–73.

Julian, F. J., J. W. Moore, and D. E. Goldman. 1962. Current-voltage relations in the lobster giant axon membrane under voltage clamp conditions. *J. Gen. Physiol.* 45:1217–1238.

Meves, H., N. Rubly, and D. D. Watt. 1982. Effect of toxins isolated from the venom of the scorpion *Centruroides sculpturatus* on the Na currents of the node of Ranvier. *Pflügers Arch. Eur. J. Physiol.* 393:56–62.

Moore, J. W., and E. B. Cox. 1976. A kinetic model for the sodium conductance system in squid axon. *Biophys. J.* 16:171.

Mozhayeva, G. N., A. P. Naumov, E. D. Nosyreva, and E. V. Grishin. 1980. Potential-dependent interaction of toxin from venom of the scorpion *Buthus eupeus* with sodium channels in myelinated fiber. *Biochim. Biophys. Acta.* 597:587–602.

Narahashi, T., J. W. Moore, and B. I. Shapiro. 1969. Condylactis toxin: interaction with nerve membrane ionic conductance. *Science (Wash. DC).* 163:680–681.

Narahashi, T., B. I. Shapiro, T. Deguchi, M. Scuka, and C. M. Wang. 1972. Effects of scorpion venom on squid axon membranes. *Am. J. Physiol.* 222:850–857.

Neumcke, B., W. Schwarz, and R. Stämpfli. 1980. Modification of sodium inactivation in myelinated nerve by *Anemonia* toxin II and iodate. *Biochim. Biophys. Acta.* 600:456–466.

New, W., and W. Trautwein. 1972. Inward membrane currents in mammalian myocardium. *Pflügers Arch. Eur. J. Physiol.* 334:1–23.

Okamoto, H. 1980. Binding of scorpion toxin to sodium channels *in vitro* and its modification by β-bungarotoxin. *J. Physiol. (Lond.).* 299:507–520.

Oxford, G. S., C. H. Wu, and T. Narahashi. 1978. Removal of sodium channel inactivation in squid giant axons by N-bromoacetamide. *J. Gen. Physiol.* 71:227–247.

Pelhate, M., B. Hue, and D. B. Sattelle. 1979. Pharmacological properties of axonal sodium channels in the cockroach *Periplaneta americana* L. *J. Exp. Biol.* 83:49–58.

Rathmayer, W., and L. Beress. 1976. The effect of toxins from *Anemonia sulcata* (Coelenterata) on neuromuscular transmission and nerve action potentials in the crayfish *(Astacus leptodactylus). J. Comp. Physiol.* 109:373–382.

Romey, G., J. P. Abita, H. Schweitz, G. Wunderer, and M. Lazdunski. 1976. Sea anemone toxin: a tool to study molecular mechanisms of nerve conduction and excitation-secretion coupling. *Proc. Natl. Acad. Sci. USA.* 73:4055–4059.

Romey, G., R. Chicheportiche, M. Lazdunski, H. Rochat, F. Miranda, and S. Lissitzky. 1975. Scorpion neurotoxin—a presynaptic toxin which affects both Na$^+$ and K$^+$ channels in axons. *Biochem. Biophys. Res. Commun.* 64:115–121.

Shapiro, B. I., and G. Lilleheil. 1969. The action of anemone toxin on crustacean neurons. *Comp. Biochem. Physiol.* 28:1225–1241.

Shrager, P. 1974. Ionic conductance changes in voltage-clamped crayfish axons at low pH. *J. Gen. Physiol.* 64:666–690.

Stengelin, S., and F. Hucho. 1980. Radioactive labelling of toxin I from *Anemonia sulcata* and binding to crayfish nerve *in vitro*. *Hoppe-Seyler's Z. Physiol. Chem.* 361:577–585.

Tamkun, M. M., and W. A. Catterall. 1981. Reconstitution of the voltage-sensitive sodium channel of rat brain from solubilized components. *J. Biol. Chem.* 256:11457–11463.

Vincent, J. P., M. Balerna, J. Barhanin, M. Fosset, and M. Lazdunski. 1980. Binding of sea anemone toxin to receptor sites associated with gating system of sodium channel in synaptic nerve endings *in vitro*. *Proc. Natl. Acad. Sci. USA.* 77:1646–1650.

Warashina, A., S. Fujita, and M. Satake. 1981. Potential-dependent effects of sea anemone toxins and scorpion venom on crayfish giant axon. *Pflügers Arch. Eur. J. Physiol.* 391:273–276.

Yeh, J. Z., G. S. Oxford, C.H. Wu, and T. Narahashi. 1976. Dynamics of aminopyridine block of potassium channels in squid axon membrane. *J. Gen. Physiol.* 68:519–535.